ARTICLE

OBC
www.rsc.org/obc

Molecular mechanism of dielectrically controlled optical resolution (DCR)

Kenichi Sakai,*[a] Rumiko Sakurai,[a] Toshio Akimoto[b] and Noriaki Hirayama*[b]

[a] *R&D Division, Yamakawa Chemical Industry Co., Ltd., Kitaibaraki, Ibaraki, 319-154, Japan*

[b] *Basic Medical Science and Molecular Medicine, Tokai University School of Medicine, Isehara, Kanagawa, 259-1193, Japan. E-mail: hirayama@is.icc.u-tokai.ac.jp*

Received 19th August 2004, Accepted 10th November 2004
First published as an Advance Article on the web 13th December 2004

We have recently found the first example of dielectrically controlled optical resolution (DCR). By adjusting the dielectric constant of the solvent used in the resolution process, each optical isomer of (*R*,*S*)-α-amino-ε-caprolactam can be selectively obtained using *N*-tosyl-(*S*)-phenylalanine as a chiral selector. The molecular mechanism of DCR has been investigated by comparing the molecular and crystal structures of the optical selector, its target substrate and their diastereomeric salts. Strong hydrophobic interactions between the phenyl rings of the optical selector govern the molecular aggregation of the selectors and form a hydrophilic layer in which molecular recognition takes place. The recognition site in the hydrophilic layer can inherently identify both of the isomers. The dielectric constant of the solvent used in the discrimination process controls the intermolecular interaction which determines the isomer to be selected. The molecular mechanism of DCR disclosed in this study strongly suggests that DCR is not a specific but a general phenomenon. This method can be applicable to a large variety of optical resolution processes.

Introduction

Diastereomeric salt formation using a resolving agent as a chiral selector is one of the most useful methods to obtain a target stereoisomer from its racemic mixture.[1] It is widely believed that the chiral discrimination process is solely dependent on the stereochemistry of the relevant molecules. No special attention has been given to the effect of the solvent properties used in the process of discrimination.

We have recently found the first example of chiral discrimination controlled by the dielectric constants (ε) of the solvents used.[2,3] In the resolution process of (*R*,*S*)-α-amino-ε-caprolactam (**1**) with *N*-tosyl-(*S*)-phenylalanine (**2**), high optical yields for (*R*)- and (*S*)-**1** can be attained simply by adjusting the dielectric constants of the solvents employed (Fig. 1). (*S*)-**1** is preferentially selected in the solvents with ε between 27 and 62. In solvents with ε lower than 27, (*R*)-**1** is exclusively precipitated. For instance, (*S*)-**1** is selectively obtained (93%) from a methanol solution (ε = 33) and (*R*)-**1** (92%) from a 2-propanol–water (89 : 11) solution (ε = 25). This phenomenon, designated as dielectrically controlled optical resolution (DCR), is very useful from the industrial point of view.

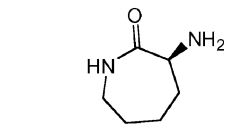

(*S*)-**1**

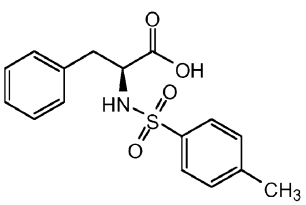

(*S*)-**2**

Fig. 1 Chemical structures of (*S*)-**1** and (*S*)-**2**.

It is very likely that the clues to this phenomenon are found in the crystal structures of both diastereomeric salts. We have successfully obtained single crystals of these salts and their component molecules. In this paper the molecular mechanisms of DCR will be discussed based on these crystal structures. The crystals of the diastereomeric salts between (*R*)-**1** and (*S*)-**2**, and (*S*)-**1** and (*S*)-**2** are designated as (*R*)-**1**:(*S*)-**2** and (*S*)-**1**:(*S*)-**2**, respectively. The crystals of (*R*)-**1** and (*S*)-**2** themselves are designated as (*R*)-**1**:(*R*)-**1** and (*S*)-**2**:(*S*)-**2**, respectively.

Results and discussion

Molecular structures of (*S*)-2

An ORTEP III[4] drawing of the molecular structure of (*S*)-**2** in the (*R*)-**1**:(*S*)-**2** salt is shown in Fig. 2 together with the atomic numbering and labeling of ring systems. Selected geometrical

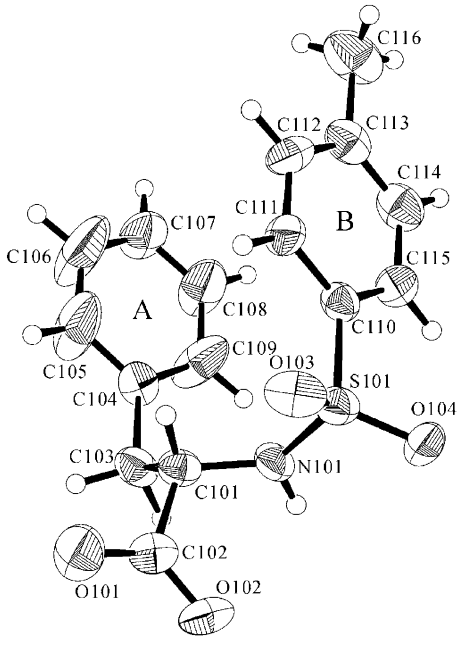

Fig. 2 Structure of (*S*)-**2** in the crystal of (*R*)-**1**:(*S*)-**2** with the atomic and ring labelling systems (drawn with ORTEP-III[4]).

DOI: 10.1039/b412827c

Table 1 Selected geometrical parameters for (*R*)-**1**:(*S*)-**2**, (*S*)-**1**:(*S*)-**2**, (*S*)-**2**:(*S*)-**2** and (*R*)-**1**:(*R*)-**1**

	(*R*)-**1**:(*S*)-**2**	(*S*)-**1**:(*S*)-**2**	(*S*)-**2**:(*S*)-**2**	(*R*)-**1**:(*R*)-**1**
(i) Torsion angles (°) in **2**				
C111–C110–S101–N101	96.9(4)	112.2(7)	87.4(4)	
C110–S101–N101–C101	−92.1(4)	−71.2(6)	−67.9(3)	
S101–N101–C101–C103	143.3(4)	146.3(5)	112.2(3)	
N101–C101–C103–C104	−72.5(6)	−73.4(8)	179.0(3)	
C101–C103–C104–C105	−89.1(7)	−58.2(11)	69.5(5)	
(ii) Dihedral angles (°) between phenyl rings and the distances (Å) between the centroids of the rings				
A/B	11.3(4)	2.6(5)	73.1(2)	
Cg(A) · · · Cg(B)[a]	4.099	4.305	6.403	
(iii) Torsion angles (°) in **1**				
N1–C2–C3–C4	60.7(6)	−70.9(9)		66.4(4)
C2–C3–C4–C5	−81.3(5)	82.0(7)		−80.1(4)
C3–C4–C5–C6	63.7(6)	−59.3(8)		61.8(5)
C4–C5–C6–C7	−59.8(5)	61.3(6)		−61.7(5)
C5–C6–C7–N1	73.7(6)	−79.2(5)		77.1(5)
C6–C7–N1–C2	−66.7(7)	64.0(10)		−63.3(6)
C7–N1–C2–C3	6.9(8)	3.6(12)		−1.3(6)
N1–C2–C3–N3	−177.7(4)	165.1(6)		−171.8(3)
O2–C2–C3–N3	3.2(7)	−16.9(10)		9.7(4)
O2–C2–C3–C4	−118.5(5)	107.2(8)		−112.0(4)

[a] Cg denotes the centroid of the phenyl ring.

parameters characterizing the conformations in the three different crystal structures are given in Table 1. The bond lengths and angles in these three molecules agree within experimental errors and all of them are within normal ranges. The chain moieties connecting the two phenyl rings have different conformations in the three molecules as indicated by the torsion angles. The molecule in the crystal of (*S*)-**2**:(*S*)-**2** adopts the most extended conformation, whereas the molecule in the (*S*)-**1**:(*S*)-**2** crystal adopts the most folded conformation. The two rings in the (*S*)-**1**:(*S*)-**2** crystal are almost parallel, whereas they are nearly perpendicular to each other in the (*S*)-**2**:(*S*)-**2** crystal. These results indicate that (*S*)-**2** is a relatively flexible molecule and can adapt its conformation to different crystalline environments.

In spite of the conformational differences, the two phenyl rings are located on the same side of the interconnecting chains in the crystal structures of (*S*)-**1**:(*S*)-**2**, (*R*)-**1**:(*S*)-**2** and (*S*)-**2**:(*S*)-**2**. The common orientation of the phenyl rings plays an important role in the formation of distinct hydrophobic layers in the crystals as described below.

Molecular structures of (*R*)-1 and (*S*)-1 molecules

An ORTEP III drawing of the molecular structure of (*R*)-**1** in the (*R*)-**1**:(*S*)-**2** salt together with the atomic numbering system is shown in Fig. 3. Selected torsion angles for (*S*)-**1** and (*R*)-**1** in the (*R*)-**1**:(*S*)-**2** (*S*)-**1**:(*S*)-**2** and (*R*)-**1**:(*R*)-**1** crystals are shown in Table 1. The absolute values of corresponding torsion angles in the three molecules are similar. This structural similarity indicates that the (*S*)-**1** and (*R*)-**1** molecules assume a relatively rigid chain conformation which is maintained in different environments. The bond lengths and angles in the three molecules agree well and are within the expected ranges.

Crystal structures of (*R*)-1:(*S*)-2, (*S*)-1:(*S*)-2 and (*S*)-2:(*S*)-2

These crystal structures drawn with the program WebLab Viewer Pro[5] are shown in Figs. 4–6. As shown in Fig. 4, four (*S*)-**2** molecules, labeled a, b, c and d, build a basic packing unit that is very similar in the three crystal structures.

The phenyl rings of (*S*)-**2** pack together and form hydrophobic layers. In the crystal of (*S*)-**2**:(*S*)-**2**, the rings A and B pack together between molecules. In the crystal structures of (*S*)-**1**:(*S*)-**2** and (*R*)-**1**:(*S*)-**2**, however, only rings B are involved in intermolecular contacts. Since the pattern of hydrophobic packing in these crystals is essentially the same, it seems that the packing between the phenyl rings is crucial in building up the three crystal structures. Between these hydrophobic layers the hydrophilic layers are formed. The molecular recognition between (*S*)-**2** and, (*R*)-**1** or (*S*)-**1**, essentially takes place in the hydrophilic layers.

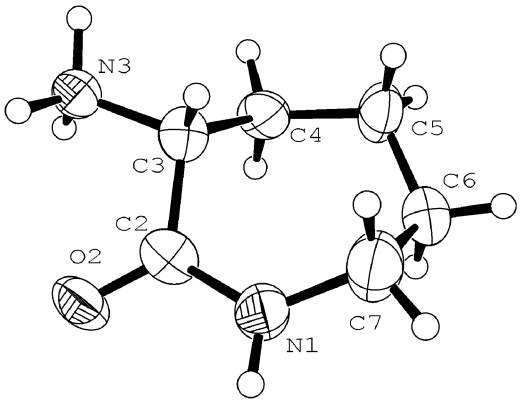

Fig. 3 Structure of (*R*)-**1** in the crystal of (*R*)-**1**:(*S*)-**2** with the atomic numbering system.

The intermolecular hydrogen bonds play decisive roles in determining the crystal packing in the hydrophilic layers. The geometrical parameters of the hydrogen bonds in these crystals are given in Table 2. Although the hydrogen bonding patterns observed between (*S*)- or (*R*)-**1** and (*S*)-**2** molecules in the (*S*)-**1**:(*S*)-**2** and (*R*)-**1**:(*S*)-**2** crystals are essentially similar, more extended hydrogen bonds are formed in (*S*)-**1**:(*S*)-**2**. In the (*S*)-**2**:(*S*)-**2** crystal, however, there are only two intermolecular hydrogen bonds.

As described above, both (*S*)-**1**:(*S*)-**2** and (*R*)-**1**:(*S*)-**2** crystals have similar packing patterns. The major difference is observed in the hydrophilic layers. In (*S*)-**1**:(*S*)-**2** the hydrophilic layer is significantly expanded and the water molecules contribute to the expansion. The distance between the C102 in molecule a and the S101 atom in the molecule c just across the hydrophilic layer seem to be a good measure to compare the width of the hydrophilic layer. These distances are 9.42 and 7.89 Å, in (*S*)-**1**:(*S*)-**2** and

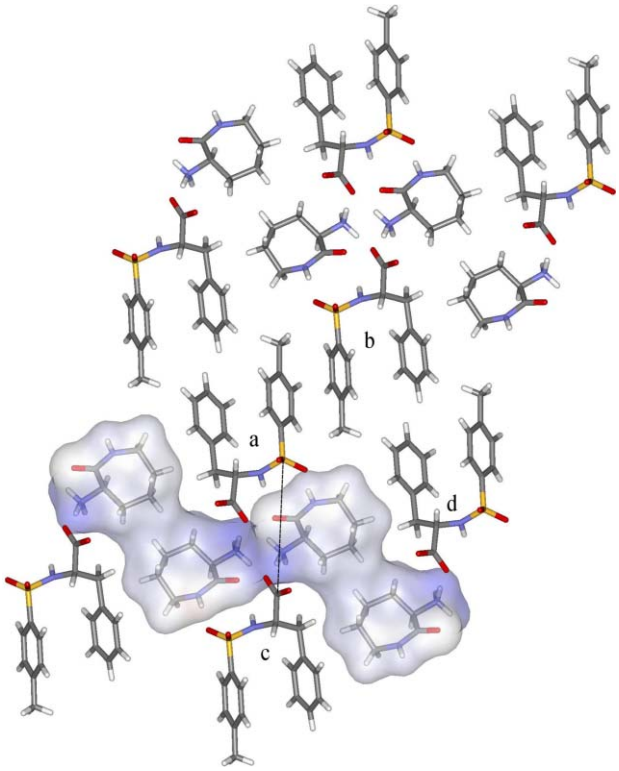

Fig. 4 Crystal structure of (*R*)-**1**:(*S*)-**2**; the solvent accessible surface of a layer of (*R*)-**1** is shown.

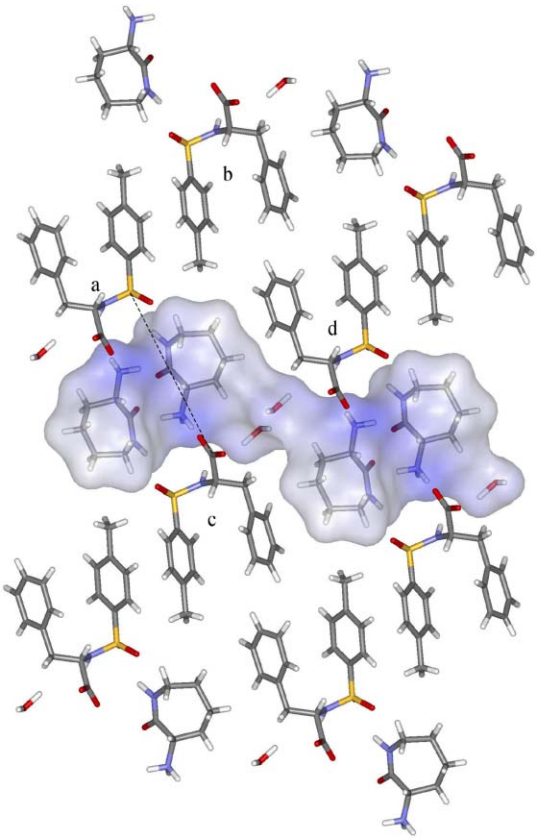

Fig. 5 Crystal structure of (*S*)-**1**:(*S*)-**2**; the solvent accessible surface of a layer consisting of (*S*)-**1** and water molecules is shown.

(*R*)-**1**:(*S*)-**2**, respectively. The solvent accessible surfaces of the hydrophilic layers are also shown in Figs. 4 and 5. The volume of the hydrophilic layers of (*S*)-**1**:(*S*)-**2** is significantly larger and accordingly the density of the (*S*)-**1**:(*S*)-**2** crystal is appreciably smaller than that of the (*R*)-**1**:(*S*)-**2**. In other words, the crystal

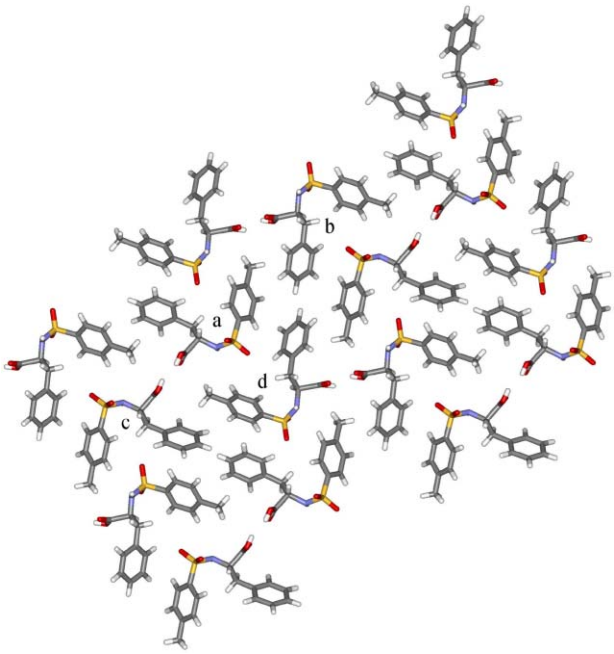

Fig. 6 Crystal structure of (*S*)-**2**:(*S*)-**2**.

of the (*S*)-**1**:(*S*)-**2** is more loosely packed than that of (*R*)-**1**:(*S*)-**2** especially in the hydrophilic layer.

Molecular mechanism of chiral discrimination

The phenyl groups of the (*S*)-**2** molecules have a pronounced tendency to aggregate and to form hydrophobic layers during crystallization. The polar groups aggregate to form hydrophilic layers between hydrophobic ones. Very similar packing patterns are observed in the crystal structures of a chiral selector (+)-(1*S*)-1,1′-binaphthalene-2,2′-diyl phosphate and several amino acids.[6] In this case the hydrophilic layers are preferentially formed and concurrently hydrophilic layers are formed. The molecular recognition between the chiral selector and the selected molecules also takes place in hydrophilic layers.

Sufficiently strong interaction between the substrate and the hydrophilic moiety of the chiral selector is required for chiral discrimination. If the dielectric constant is low, the polar groups in the hydrophilic layer can approach so close that the hydrophilic layer packs tightly. To estimate the stereochemical effect of the replacement of (*R*)-**1** by (*S*)-**1** in the crystal structure of (*R*)-**1**:(*S*)-**2**, the (*S*)-**1** molecule was superimposed to the (*R*)-**1** molecule in the crystal. Six atoms in the ring except the C3 atom are superimposed relatively well (rmsd = 0.429 Å), but as shown in Fig. 7, the difference of the stereochemistry at C3 would greatly affect hydrogen bonding in its neighborhood. If the (*R*)-**1** molecule is replaced by the (*S*)-**1** molecule, the hydrogen bond between the N3 atom and the O102 atom of the upper left (*S*)-**2** molecule in the crystal would be broken because the N3 atom no longer points towards the O102 atom of the molecule. The N3 atom instead now approaches the O102 atom of the lower left (*S*)-**2** molecule. The distance between these atoms would be too short (1.38 Å in this superposition) as a hydrogen bond and such a short contact would cause a significant steric hindrance. Since the conformational flexibility of molecule **1** is not so high, the steric hindrance would not be relieved by changing its conformation. This indicates that the (*S*)-**1** molecule cannot be accommodated in such a crystal structure and the lower left (*S*)-**2** molecule should shift away at least 1 Å to accommodate the (*S*)-**1** molecule. The shift implies an expansion of the hydrophilic layer. If the dielectric constant of the solvent is low, such an expansion is impossible. Therefore under the situation, only the (*R*)-**1** isomer can be discriminated.

Table 2 Hydrogen bonds[a]

D–H···A	Symmetry code	D–H/Å	H···A/Å	D···A/Å	D–H···A/°
(*S*)-**1**:(*S*)-**2**					
N3–H···O2	$1-x, -1/2+y, -z$	0.98	1.97	2.791(7)	139
N3–H···O102	$1-x, -1/2+y, -z$	0.95	1.88	2.686(8)	141
N3–H···O101	$1-x, 1/2+y, -z$	0.99	2.19	2.813(7)	119
N3–H···O102	$1-x, 1/2+y, -z$	0.99	2.23	3.221(8)	175
O6–H···O6[b]	$2-x, -1/2+y, -z$	0.92	2.06	2.868(8)	146
N101–H···O101	$x, 1+y, z$	0.74	2.09	2.811(7)	165
N1–H···O103	x, y, z	1.10	1.91	2.902(8)	148
O6–H···O101	$1+x, y, z$	1.11	1.75	2.777(8)	151
(*R*)-**1**:(*S*)-**2**					
N1–H···O104	$x, 1+y, z$	0.87(5)	2.14(5)	3.007(6)	177(4)
N3–H···O102	$2-x, 1/2+y, 1-z$	0.95	1.78	2.721(5)	168
N3–H···O102	x, y, z	0.95	1.78	2.725(5)	171
N3–H···O101	$2-x, -1/2+y, 1-z$	0.95	2.07	2.926(5)	149
(*S*)-**2**:(*S*)-**2**					
O101–H···O102	$1/2+x, 3/2-y, 1-z$	0.80(5)	1.92(5)	2.676(4)	157(5)
N101–H···O103	$-1+x, y, z$	0.75(4)	2.33(4)	3.060(6)	165(4)

[a] A and D denote hydrogen bond acceptor and donor, respectively. [b] O6 designates the oxygen atom of the water molecule.

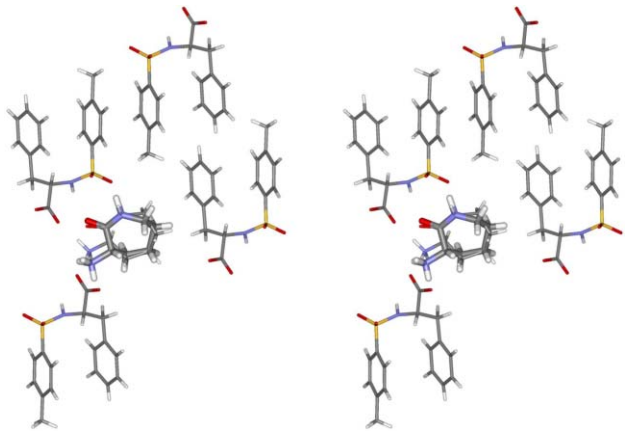

Fig. 7 Stereoscopic drawing of a part of the crystal structure of (*R*)-**1**:(*S*)-**2**. An (*S*)-**1** molecule is superimposed on the (*R*)-**1** molecule. The former molecule is drawn with thick sticks.

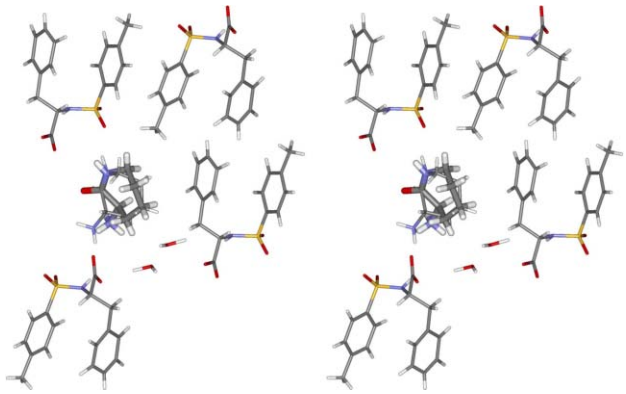

Fig. 8 Stereoscopic drawing of a part of the crystal structure of (*S*)-**1**:(*S*)-**2**. An (*R*)-**1** molecule is superimposed on the (*S*)-**1** molecule. The former molecule is drawn with thick sticks.

Under the condition of medium dielectric constant, the interaction between the polar groups would be shielded to some extent and the hydrophilic layer can expand. Such an expansion is realized in the crystal of (*S*)-**1**:(*S*)-**2**. Expansion of the hydrophilic layer, however, means that the crystal packing gets worse and the efficiency of the discrimination drops. In the (*S*)-**1**:(*S*)-**2** crystal, this problem is solved by a water molecule incorporated into the hydrophilic layer. The water molecule fills the void and realizes a relatively close packing. To understand the reason why the (*R*)-**1** molecule can not be discriminated in this case, the (*R*)-**1** molecule was superimposed to the (*S*)-**1** molecule in this crystal using a similar condition as described above (r.m.s.d. = 0.430 Å). As shown in Fig. 8 the hydrogen bond between the N1 atom and the O103 atom of the upper left (*S*)-**2** molecule is maintained. The N3 atom in (*R*)-**1**, however, is moved away from the O102 atom of the lower left (*S*)-**2** molecule and the hydrogen bond between these atoms in the (*S*)-**1**:(*S*)-**2** crystal is disrupted. The N3 atom now points toward the water molecule, but the distance (N···O 3.68 Å) is too long for a hydrogen bond. The replaced (*R*)-**1** molecule would be only loosely recognized here at this recognition site. This implies that under the condition of medium dielectric constant the (*R*)-molecule will not be fixed there and cannot be discriminated properly given the (*S*)-**2** molecules adopts this particular packing pattern.

Conclusions

In a solvent with low dielectric constant, the electrostatic interactions between polar groups of the relevant molecules are weakened and they can approach closely. Under such a situation, (*R*)-**1** should be preferable to pack the hydrophilic layers efficiently. Due to this reason, (*R*)-**1**:(*S*)-**2** crystals were obtained from a solvent system with ε of 5. On the other hand, in a solvent system with medium dielectric constant, the polar groups should be separated enough. Under such circumstances a water molecule is necessary to maintain the close packing of the hydrophilic layer. The situation makes it possible that (*S*)-**1** is preferentially discriminated. Therefore (*S*)-**1**:(*S*)-**2** crystals were obtained from the solvent system with ε of 38.

The crystal structures of (*R*)-**1**:(*S*)-**2** and (*S*)-**1**:(*S*)-**2** unequivocally show that the hydrophilic layers formed in these crystals can inherently accommodate both (*R*)-**1** and (*S*)-**1** isomers. Discrimination of one of the isomers may be a matter of selecting the suitable intermolecular hydrogen bonds between the chiral selector and the isomer to be discriminated. This study strongly suggests that the selection of the intermolecular hydrogen bonds

Table 3 Crystallographic data

	(*R*)-**1**:(*S*)-**2**	(*S*)-**1**:(*S*)-**2**	(*S*)-**2**:(*S*)-**2**	(*R*)-**1**:(*R*)-**1**
Formula	$C_{22}H_{29}N_3O_5S$	$C_{22}H_{29}N_3O_5S{\cdot}H_2O$	$C_{16}H_{17}NO_4S$	$C_6H_{13}N_2OCl$
Solvent	Chloroform	Ethanol	Ethanol	Ethanol
Space group	$P2_1$	$P2_1$	$P2_12_12_1$	$P2_12_12_1$
Crystal system	Monoclinic	Monoclinic	Orthorhombic	Orthorhombic
Formula weight	447.55	465.56	319.37	164.63
a/Å	11.2302(4)	12.723(1)	5.212(4)	5.0426(6)
b/Å	5.5390(2)	5.3119(3)	13.5426(8)	7.6092(7)
c/Å	17.850(2)	17.908(1)	22.162(2)	21.615(3)
β/°	95.444(2)	100.305(3)		
V/Å^3	1105.4(1)	1190.8(2)	1564(1)	829.4(2)
Z	2	2	4	4
D_c/g cm^{-3}	1.345	1.298	1.356	1.318
μ/mm^{-1}	1.630	1.565	1.997	3.588
F(000)	476	496	672 352	
T/K	293(1)	293(1)	293(1)	293(1)
$2\theta_{max}$/°	136.4	136.4	136.1	136.4
Total reflections measured	24356	26744	32768	18438
Symmetry independent reflections [$F^2 > 2\sigma(F^2)$]	3851	3818	2805	1474
Observed reflections	2355	2358	2242	1228
R^a [$F^2 > 2\sigma(F^2)$]	0.067	0.080	0.056	0.046
wR^b [$F^2 > 2\sigma(F^2)$]	0.067	0.154	0.1090	0.092
Goodness of fit	1.447	1.389	0.948	0.881
Final Δ_{max}/σ	0.000	0.016	0.000	0.000
$\Delta\rho$(max.;min.)/e Å^{-3}	1.04; −0.58	0.85; −0.68	0.59; −0.50	0.52; −0.30

^{a} $R = \Sigma \| F_o| - |F_c\| / \Sigma |F_o|$. ^{b} $wR = \Sigma \{w(F_o^2 - F_c^2)^2 / \Sigma w(F_o^2)^2\}^{1/2}$; $w = 1/[0.0010F_o^2 + 3.0000\sigma(F_o^2) + 0.5000]/(4F_o^2)$.

can be controlled by adjusting the dielectric constant of the employed solvent.

The present study has successfully disclosed the molecular mechanism of the newly discovered DCR effect. Since no extraordinary molecular structures are required for chiral selectors and their substrates, the DCR is possibly not a special but a general method. This means that DCR can be expected to be applicable to a variety of optical resolution processes and might even revolutionize industrial scale optical resolution.

Experimental

Resolution and crystallization

Typical experimental procedures are as follows. Resolution results are evaluated by yield,[7] diastereomeric excess (de),[8] and resolution efficiency (E).[9]

(*S*)-1:(*S*)-2. To a 1000 mL flask were added (*R*,*S*)-**1** (50 g, 390 mmol; containing 3.7% of water), (*S*)-**2** (124.6 g, 390 mmol) and methanol (500 g), and the mixture was stirred and heated to about 55 °C to give a clear solution. The solution was then gradually cooled, seeded (2 mg) at 48 °C, kept for 1 h at 36–38 °C (corresponding to the crystallization temperature), and then cooled again to 20 °C. After aging the suspension at this temperature for 1 h, the crystals were filtered off and washed twice with methanol (20 mL in total) to afford crude (*S*)-**1**:(*S*)-**2** (52.6 g, 113 mmol, 29% yield, 93% de, E 54%). The crystal contains a water molecule of crystallization. The (*S*)-**1**:(*S*)-**2** salt was recrystallized in a 74% ethanol solution ($\varepsilon = 38$) and single crystals suitable for diffraction experiments were obtained.

(*R*)-1:(*S*)-2. The mother-liquor obtained after the first resolution described above was evaporated to dryness giving a condensate (122.3 g; 40% de). To the condensate was added 2-propanol (333 g) and water (41 g) and the slurry was transferred to a 500 mL flask. The mixture was stirred and heated to about 75 °C to give a clear solution. The solution was then gradually cooled, seeded (2 mg) at 66 °C, kept for 1 h at 62–64 °C (corresponding to the crystallization temperature), and then cooled again to 20 °C. After aging the suspension at this temperature for 1 h, the crystals were filtered off and washed twice with 89% 2-propanol (20 mL in total) to afford crude (*R*)-**1**:(*S*)-**2** (71.4 g, 160 mmol, 41% yield, 92% de, E 75%). The (*R*)-**1**:(*S*)-**2** salt was recrystallized from an absolute ethanol solution ($\varepsilon = 24$) and single crystals suitable for diffraction experiments were obtained.

The dielectric constant of the mixed solvent was calculated as a weighted average of the values of the components at 20 °C.[10]

X-Ray analysis

The single crystals of (*S*)-**1**:(*S*)-**2** were relatively small and highly fragile. All of the crystals were stable under the laboratory conditions and were mounted on glass fibers and used for data collection. The crystal data, experimental details and structure refinement are summarized in Table 3. All structures were solved by direct methods with program SIR 92[11] an refined by the full-matrix least-squares method. Non-hydrogen atoms were refined anisotropically. Most of the hydrogen atoms were obtained from difference syntheses and refined with the riding model. The absolute configurations were fixed to the known ones and not reconfirmed by the X-ray analyses independently. All of the calculations were performed using the software system CrystalStructure.[12]

CCDC reference numbers 220041, 220042, 234395 and 234396 for (*S*)-**1**:(*S*)-**2**, (*R*)-**1**:(*S*)-**2**, (*R*)-**1**:(*R*)-**1** and (*S*)-**2**:(*S*)-**2**, respectively.

See http://www.rsc.org/suppdata/ob/b4/b412827c/ for crystallographic data in CIF or other electronic format.

Acknowledgements

One of the authors (N. H.) is grateful for financial support from the Research and Study Program of Tokai University Educational System General Research Organization.

References

1 J. Jacques, A. Collet and S. H. Wilen, *Enantiomers, Racemates and Resolutions*, Wiley-Interscience, 1981, p. 251.
2 K. Sakai, R. Sakurai, A. Yuzawa and N. Hirayama, *Tetrahedron: Asymmetry*, 2003, **14**, 3713–3718.

3 K. Sakai, R. Sakurai and N. Hirayama, *Tetrahedron: Asymmetry*, 2004, **15**, 1073–1076.
4 M. N. Burnett and C. K. Johnson, *ORTEP-III: Oak Ridge Thermal Ellipsoid Plot Program for Crystal Structure Illustration*, Oak Ridge National Laboratory Report ORNL-6895, Oak Ridge, TN, 1996.
5 *WebLab ViewerPro: Version 5.0*, Molecular Simulations Inc., San Diego, CA, 2000.
6 I. Fujii and N. Hirayama, *Helv. Chim. Acta*, 2002, **85**, 2946–2960.
7 Yield (%) is calculated based on (*R*,*S*)-**1**.
8 Diastereomeric excess (% de) = [A − B] × 100(A + B), where A and B are the diastereomers.
9 Resolution efficiency, *E* (%) = yield (%) × de (%) × 2/100.
10 A. Jouyban, S. Soltanpour and H.-K. Chan, *Int. J. Pharm.*, 2004, **269**, 353–360.
11 A. Alltomare, G. Cascarano, C. Giacovazzo, A. Guagliardi, M. Burla, G. Polidori and M. Camalli, *J. Appl. Crystallogr.*, 1994, **27**, 435.
12 *CrystalStructure Ver. 3.6.0, Crystal Structure Analysis Package*, Rigaku, Tokyo, Japan and Rigaku/MSC, Texas, USA, 2004.